International Journal of Nanomedicine

Dovepress
open access to scientific and medical research

Open Access Full Text Article

ORIGINAL RESEARCH

The Self-Assembly Soluplus Nanomicelles of Nobiletin in Aqueous Medium Based on Solid Dispersion and Their Increased Hepatoprotective Effect on APAP-Induced Acute Liver Injury

Jinrong Ning[1,*], Guodong Zheng[1,*], Yi Cai[1,*], Yunguang Hu[2,*], Yiqi Liu[1], Enping Lai[1], Baizhong Chen[3], Yujie Liu[1], Ziqi Liang[1], Jijun Fu[1], Minyan Wei[1]

[1]Key Laboratory of Molecular Target & Clinical Pharmacology and the State Key Laboratory of Respiratory Disease, School of Pharmaceutical Sciences & The Fifth Affiliated Hospital, Guangzhou Medical University, Guangzhou, 511436, People's Republic of China; [2]Medical Department, Guangdong Yifang Pharmaceutical Co., Ltd, Foshan, Guangdong, 528200, People's Republic of China; [3]Guangdong Xinbaotang Biological Technology Co., Ltd, Jiangmen, Guangdong, 529000, People's Republic of China

*These authors contributed equally to this work

Correspondence: Minyan Wei; Jijun Fu, Guangzhou Medical University, Guangzhou, 511436, People's Republic of China, Tel +86-20-37103268, Email weiminyan@163.com; fujj@gzhmu.edu.cn

Purpose: APAP-induced liver injury (AILI) is a common cause of acute liver failure (ALF). Nobiletin (NOB) is a potential hepatoprotective agent for the treatment of APAP-induced liver injury. However, the poor solubility and low bioavailability of NOB hinders its application. In this study, a novel self-assembly nano-drug delivery system of nobiletin (solid dispersion of NOB, termed as NOB/SD) was developed based on solid dispersion technology to improve the bioavailability and hepatoprotective ability of NOB for APAP-induced liver injury therapy.

Methods: The optimized NOB/SD system was constructed using the amphiphilic copolymers of Soluplus and PVP/VA 64 via hot melt extrusion technology (HME). NOB/SD was characterized by solubility, physical interaction, drug release behavior, and stability. The bioavailability and hepatoprotective effects of NOB/SD were evaluated in vitro and in vivo.

Results: NOB/SD maintained NOB in matrix carriers in a stable amorphous state, and self-assembled NOB-loaded nanomicelles in water. Nanostructures based on solid dispersion technology exhibited enhanced solubility, improved release behavior, and promoted cellular uptake and anti-apoptosis in vitro. NOB/SD displayed significantly improved bioavailability in healthy Sprague Dawley (SD) rats in vivo. Furthermore, NOB/SD alleviated the APAP-induced liver injury by improving anti-oxidative stress with reactive oxygen species (ROS) scavenging and nuclear factor erythroid 2-related factor 2 (Nrf2) activation.

Conclusion: These results suggested that NOB/SD could be considered as a promising hepatoprotective nano-drug delivery system for attenuating APAP-induced acute liver injury with superior bioavailability and efficient hepatoprotection, which might provide an effective strategy for APAP-induced acute liver injury prevention and treatment.

Keywords: nobiletin, self-assembly micelles, solid dispersion technology, hot melt extrusion, acetaminophen-induced liver injury

Introduction

Drug-induced liver injury (DILI) is one of the most common causes of acute liver failure (ALF), which is considered a great public health problem to human beings in the world.[1,2] Among them, more than 50% of ALF cases are caused by acetaminophen (APAP) overdose worldwide, especially in the United States and parts of Europe.[3] APAP-induced liver injury (AILI) is developed to hepatocyte necrosis and acute inflammation, with intracellular reactive oxygen species (ROS) overgeneration and serum alanine aminotransferase (ALT) and aspartate transaminase (AST) increase, and finally may lead to acute liver failure or even death. To date, N-acetylcysteine (NAC) is the first-line drug for AILI treatment,

Received: 19 June 2023
Accepted: 29 August 2023
Published: 8 September 2023

Graphical Abstract

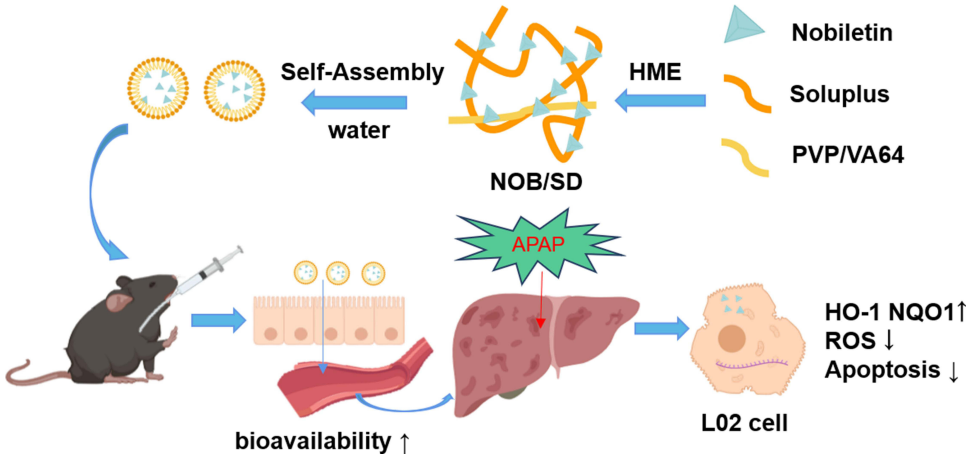

which can effectively attenuate APAP-induced hepatotoxicity by defending against oxidative stress with intracellular ROS scavenge and glutathione (GSH) supplementation in vivo.[4,5] However, adverse effects such as vomiting, gastro-esophageal reflux, and allergic reactions may occur after treatment with NAC.[6] Obviously, efficient therapies for the treatment of APAP-induced liver injury are limited in clinical practice. Therefore, effective therapeutic strategies for treating or preventing AILI are urgently needed.

Nobiletin (NOB; 5,6,7,8,3,4-hexamethoxyflavone) is a natural polymethoxylated flavone found in citrus peels that has been widely used in traditional Chinese medicine. NOB has been demonstrated to possess effective pharmacological effects on anti-inflammatory and anti-oxidative stress activities.[7] Notably, NOB ameliorates chemical and drug-induced liver injury by protecting hepatocytes from necrosis via suppressing nuclear factor-kappa B (NF-κB) activated signaling pathway to relieve oxidative stress and inflammation, which suggested that NOB might be a potential hepatoprotective candidate for the treatment of APAP-induced liver injury.[8–10] However, the poor solubility and low bioavailability of NOB hinder its further clinical application in AILI therapy.[11,12] Therefore, a novel drug delivery system is valuably developed to improve the bioavailability and hepatoprotective ability of NOB for APAP-induced liver injury therapy.[13]

Solid dispersion (SD) technology is one of the most effective techniques for drug solubility enhancement and has been widely used in the pharmaceutical industry.[14,15] In solid dispersion systems, the poorly soluble drugs are dispersed in the SD carrier (usually a hydrophilic polymer) in molecular or microcrystalline states, which might contribute to fast dissolution, enhanced solubility, and improved bioavailability of drugs.[16] At present, more than 30 pharmaceutical products based on solid dispersion technology have been approved by the US Food and Drug Administration (FDA), including apalutamide, olaparib, regorafenib, tacrolimus, etc.[17–20] Hot melt extrusion is a solvent-free and single-step technique for SD preparation, which is regarded as a sustainable and appropriate approach for commercial-scale production of SD. In our previous study, solid dispersions of nimodipine were successfully prepared by hot melt extrusion technology using Soluplus and PVP/VA 64 as carriers.[21] Interestingly, solid dispersion of nimodipine improved the solubility and bioavailability of nimodipine with Soluplus/PVP/PV 64-based micelles constructed in aqueous media. Thus, solid dispersion may be an effective strategy for enhancing the solubility of NOB. Moreover, it is hypothesized that nobiletin-loaded Soluplus nanomicelles might be self-assembled in aqueous media based on amorphous solid dispersion technology, which would exert an increased hepatoprotective effect by improving solubility in APAP-induced acute liver injury treatment.

In this study, a novel self-assembly nano-drug delivery system of nobiletin was developed based on solid dispersion technology (solid dispersion of NOB, NOB/SD, Figure 1). The optimized NOB/SD system was constructed using amphiphilic copolymers of Soluplus and PVP/VA 64 via HME. NOB/SD was characterized using scanning electron

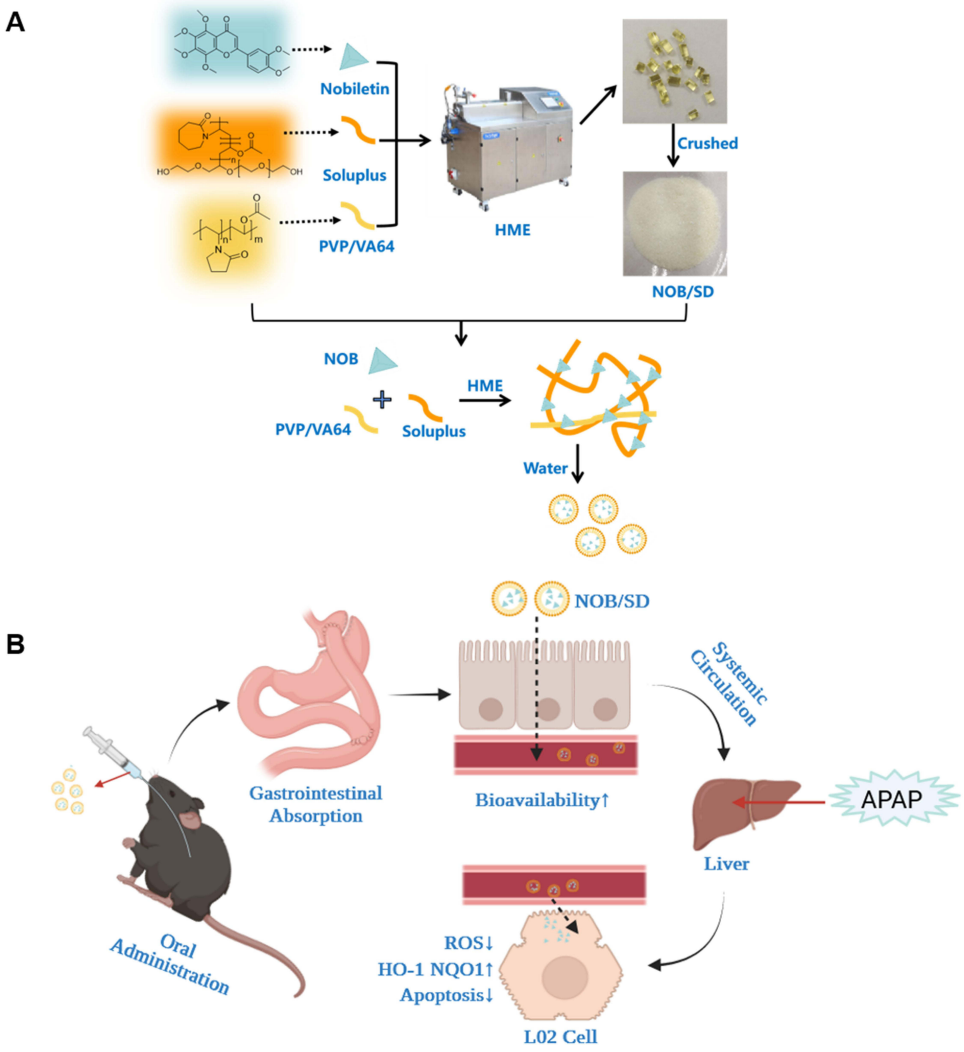

Figure 1 The schematic illustration of NOB/SD for hepatoprotective effect on APAP-induced acute liver injury. The schematic illustration of NOB/SD for hepatoprotective effect on APAP-induced acute liver injury. (**A**) The HME process of NOB/SD and its solubilization mechanism based on self-assembly Soluplus nanomicelles of NOB in aqueous medium. (**B**) The hepatoprotective mechanism of NOB/SD for APAP-induced acute liver injury treatment.

microscopy, powder X-ray diffraction, thermal analysis, and Fourier transform infrared spectroscopy. The solubility, drug release behavior, and stability of NOB/SD were evaluated, and the solubilization mechanism was clarified. The hepatoprotective effects and cytoprotective mechanisms of NOB/SD were evaluated in vitro. Furthermore, the bioavailability of NOB/SD was assessed in healthy SD rats, and the in vivo hepatoprotective effects of NOB/SD were verified in C57BL/6 mice with APAP-induced liver injury. The novel self-assembly nano-drug delivery system of nobiletin (NOB/SD) may potentially attenuate APAP-induced acute liver injury with superior bioavailability and efficient hepatoprotection and can be considered as a promising hepatoprotective nano-drug delivery system for APAP-induced acute liver injury prevention and treatment.

Materials and Methods

Materials and Reagents

Kollidon VA64 (PVP/VA 64), Polyvinylpyrrolidone (PVP K30), Kolliphor P407, and Soluplus were kindly provided by the BASF Corporation (Shanghai, China). Hydroxypropyl cellulose (HPC) was kindly provided by Japan Caoda Co., Ltd. (Hong Kong, China). Hydroxypropyl methylcellulose (HPMC) and Hypromellose acetate succinate (HPMCAS) were

kindly provided by Shin-Etsu Chemical Co., Ltd. (Tokyo, Japan). β-Cyclodexrtin (β-CD) was purchased from Macklin Biochemical Co., Ltd. (Shanghai, China). The reference standard of nobiletin (NOB) was obtained from Weikeqi (Sichuan, China) with purity higher than 98%.

The human hepatocyte cell line L02 cells were purchased commercially from the Cell Bank of Chinese Academy of Sciences (Shanghai, China). Roswell Park Memorial Institute 1640 medium (RPMI 1640), fetal bovine serum (FBS), penicillin-streptomycin, and pancreatic enzymes were all purchased from Gibco (California, USA). MTT was purchased from Solarbio (Beijing, China). The green fluorescent dye coumarin 6 (C6) was purchased from Aladdin (Sichuan, China). DCFH-DA reagent and the Annexin V-FITC/PI Apoptosis Detection Kit were obtained from Beyotime (Shanghai, China). The DAPI reagent was purchased from Beibo (Shanghai, China). Both the PrimeScript™ RT Reagent Kit and ChamQ Universal SYBR qPCR Master Mix were purchased from TaKaRa (Dalian, China).

Healthy male Sprague Dawley (SD) rats (weighted 180–220 g) and male C57BL/6 mice (weighted 18–22 g) were purchased from Guangdong Zhiyuan Biopharmaceutical Technology Co., Ltd. (Guangzhou, China). All animal experiments were approved by the Institutional Animal Care and Use Committee of Guangzhou Medical University (permission number SQ2021-024). Animal welfare and experimental procedures were performed in accordance with the rules of Committee on Animal Research and Ethics of Guangzhou Medical University. Laboratory animals were maintained in a daily cycle of 12-hour light/12-hour darkness with the humidity of 60 ± 5%, the temperature of 22 ± 2 °C, and free access to regular diets and water.

The NOB Solubility Tests in Different Polymers

NOB solubility tests were performed on eight different polymers. Briefly, 10 mg of polymers including HPC, HPMC, HPMCAS, Kolliphor P407, β-CD, Soluplus, PVP K30, and PVP/VA 64 were dissolved into 25 mL of deionized water, respectively. Then, 3.5 mg of NOB in 150 μL of ethanol was quickly added into the above polymer media, and the NOB ethanol solution was added in water as the negative control.[22] The mixtures were shaken at 100 rpm and 37 °C in an electrical shaker for 5 h. Subsequently, 4 mL of the withdrawn samples were filtered through a 0.45 μm filter. NOB concentrations in the samples were measured using an Evolution 300 UV-visible spectrophotometer at 330 nm (Thermo Fisher, Massachusetts, USA).[22]

Preparation of NOB/SD

Solid dispersions of NOB (NOB/SD) were prepared by the solvent evaporation method. The NOB formulations are shown in Table 1. Briefly, NOB and the polymers were dissolved in 40 mL of ethanol and mixed under ultrasonication at 25 °C for 10 min. Subsequently, the mixture was dried at 80 °C for 24 h and then quickly cooled down at −20 °C for 12

Table 1 NOB/SD Formulations Prepared by Different Kinds of Carriers, Ratios of NOB/Carriers and Preparation Methods

Formulation	Carriers in NOB/SD	Ratio of NOB/Carriers (Mass Ratio)	Preparation Method
1	NOB:PVP/VA 64	1:6	SE
2	NOB:HPC	1:6	SE
3	NOB:Kolliphor P407	1:6	SE
4	NOB:Soluplus	1:6	SE/HME
5		1:3	SE
6		1:2	SE
7	NOB:Soluplus:PVP/VA 64	1:5.5:0.5	SE
8		1:5:1	SE/HME
9		1:4:2	SE
10		1:3:3	SE

Abbreviations: SE, solvent evaporation technology; HME, hot melt extrusion technology.

h. Finally, the NOB/SD was obtained and sieved through an 80-mesh sieve. NOB/SD was stored at room temperature until further use.

Coumarin 6 labeled solid dispersion with a coumarin 6/SD ratio of 1:5000 was prepared with the same solvent evaporation method. Briefly, coumarin 6 and polymers (1:5000 mass ratios) were dissolved in 20 mL of ethanol and kept at 80 °C until dried. Then, the dried mixture was quickly cooled down at −20 °C for 12 h. The coumarin 6 labeled solid dispersion (C6/SD) was obtained.

Optimized formulations of NOB (NOB/SD) were prepared using hot melting extrusion technology. Briefly, NOB was homogenously mixed with polymers (Table 1) at different ratios, respectively. The mixture was fed into a HAAKE MiniCTW extruder (Thermo, Germany) with an extrusion temperature of 170 °C. After HME treatment within 15 min, the extrudates were cooled down to room temperature, followed with the mill to pass through an 80-mesh sieve. NOB/SD values were obtained for further use.

The NOB Solubility Assay in Different NOB/SD Formulations

The solubility of NOB in the different solid dispersions was also measured. Briefly, 30 mg of NOB/SD samples were added to 10 mL of water and then shaken for 6 h in a shaker at 100 rpm and 37 °C, respectively. At the time intervals, the samples were collected and filtered with a 0.45 μm PVC membrane. Finally, the filtrates were diluted with ethanol and analyzed by UV method at 330 nm.

Characterization of NOB/SD

The optimized formulations of NOB/SD were analyzed by scanning electron microscopy (SEM). SEM images of NOB/SD were obtained using a SU8010 scanning electron microscope (Hitachi, Tokyo, Japan). The glass transition temperature (Tg) of NOB/SD was determined by differential scanning calorimetry (DSC) using a 214 Polyma DSC analyzer (Netzsch, Bavaria, Germany). DSC data were collected at a heating rate of 5 °C/min from 30 °C to 210 °C.[20] The optimized NOB/SD formulation was analyzed by powder X-ray diffraction (PXRD). The PXRD curves of the NOB-based formulations were obtained using an Empyrean PXRD system (PANalytical, Almelo, Netherlands) with Copper-kα radiation (40 kV, 30 mA). The optimized NOB/SD formulation was analyzed using Fourier transform infrared spectroscopy (FTIR) with a pressed KBr pellet. Fourier transform infrared (FTIR) spectra were recorded using a Nicolet 6700 spectrometer (ThermoFisher, Massachusetts, USA) ranging from 400 to 4000 cm^{-1}.

The mechanism of NOB solubility enhancement in NOB/SD was performed as follows. The morphology of the NOB/SD in water was characterized using a JEM 2100 transmission electron microscope (TEM) (JOEL, Japan). The particle size of NOB/SD in water was analyzed by dynamic light scattering (DLS) using a Malvern Zetasizer Nano sizer (Malvern, UK). The absorption of NOB/SD in water and methanol was measured using an Evolution 300 UV-visible spectrometer (Thermo Fisher, Massachusetts, USA) at wavelengths ranging from 200 to 450 nm. The nuclear magnetic resonance hydrogen spectrum (1H-MNR) of NOB/SD was detected by a JNM-ECZ400S/L1 Nuclear magnetic resonance spectrometer (JOEL, Japan).

In vitro Release Assay

An in vitro release assay of NOB/SD was performed using a dissolution test. Briefly, the optimized NOB/SD formulations and Free NOB (30 mg NOB) were added to the release mediums (pH 6.5 PBS, 500 mL) and shaken at 200 rpm at 37 °C for 2 h. At certain time intervals, 4 mL of the release medium was withdrawn, and equivalent PBS volumes were immediately added. After filtered through 0.45 μm filter membranes, the samples were diluted with methanol and measured by UV at 330 nm.

Stability of NOB/SD

The NOB/SD formulations (No.4 and 8) were prepared by HME and stored at 25 °C for 3 months. Physicochemical characteristics of the NOB/SD formulations were measured using DSC and in vitro release assays. Free NOB, SD carriers, NOB/PM and NOB/SD formulations without storage were used as the controls.

Cell Culture

L02 human normal liver cells were cultured in RPMI 1640 with 10% FBS, 100 U/mL penicillin and 100 mg/mL streptomycin. L02 cells were maintained at 37 °C in a humidified atmosphere containing 5% CO_2.

Cellular Uptake Study

Cellular uptake of coumarin 6 labeled NOB/SD in L02 cells was performed using confocal laser scanning microscopy (CLSM). L02 cells at a density of 1×10^5 cells/well were seeded in confocal dishes and incubated overnight. Subsequently, L02 cells were treated with C6/SD or Free C6 (at a C6 concentration of 10 nM) for 4 h. The cells were washed with PBS and fixed with 4% paraformaldehyde for 15 min. Afterwards, cells were stained and incubated with DAPI for 15 min in dark. Finally, the cellular uptake behavior of C6/SD cells was observed using A1+ confocal laser scanning microscope (CLSM, Nikon, Japan).

MTT Assay

The cell viabilities of NOB/SD were performed using MTT assay. The L02 cells were cultured in 96-well plates at a density of 5×10^3 cells/well. After incubation for 24 h, L02 cells were treated with NOB/SD or Free NOB at various NOB concentrations ranging from 0 to 12 μM for 24 h, followed by APAP (7.5 mM) treatment for another 24 h. Then, 20 mL MTT (5 mg/mL) was added and cells were incubated for 4 h. Finally, Formazan crystals in each well were dissolved in DMSO (100 μL per well), and the absorbance was measured at 492 nm using an Epoch microplate reader (BioTek, Vermont, USA).[23,24] Cells without APAP treatment were also performed using the same procedures described above.

Annexin V/PI Staining

The cell apoptosis of NOB/SD was evaluated using Annexin V/PI staining. L02 cells at a density of 5×10^5 cells/well were seeded in six-well plates and incubated overnight. After pre-incubation with NOB/SD or Free NOB (at a NOB concentration of 12 μM) for 12 h, the L02 cells were treated with APAP (7.5 mM) for 24 h. The treated L02 cells were collected, washed twice with PBS, resuspended in PBS, and stained using the Annexin V-FITC/PI Apoptosis Detection Kit according to the manufacturer's instructions. The apoptosis rates of the cells were detected using a CytoFLEX S.4 flow cytometer (Beckman Coulter, USA).

Reactive Oxygen Species (ROS) Measurement

L02 cells at a density of 1×10^6 cells/well were seeded in six-well plates and incubated overnight. The L02 cells were incubated with NOB/SD or Free NOB (NOB: 12 μM) for 4 h, followed by treatment with APAP (7.5 mM) for 24 h. Subsequently, the treated L02 cells were exposed to DCFH-DA for 30 min. The levels of ROS were detected by the CLSM.

Quantitative Real-Time PCR Analysis

L02 cells at a density of 1×10^6 cells/well were seeded in six-well plates and cultured overnight. After incubation with NOB/SD or Free NOB at NOB concentrations of 12 μM for 24 h, the treated L02 cells were exposed with 7.5 mM APAP for another 24 h. Total RNA was extracted using TRIzol (Thermo, Massachusetts, USA) and converted into cDNA using a reverse transcription kit (Vazyme, Nanjing, China) according to the manufacturer's protocols. The RNA expression levels of HO-1 and NQO1 were analyzed using quantitative real-time PCR system (Bio-Rad, USA).[25] The primers in the reaction are shown in Table 2.

In vivo Pharmacokinetic Study

Healthy male SD rats (180–220 g) were randomly divided into two groups (n = 3 per group). Then, the SD rats were orally administrated with NOB/SD and Free NOB with the NOB concentration of 50 mg/kg, respectively.[9] At time intervals, blood samples were collected from tail vein after drug administration.

Table 2 The Primer Sequences for qPCR to Assess the Expression of HO-1, NQO1 and GAPDH in L02 Cells

Target	Primer	Sequence
GAPDH	FP	5′-CTGCACCACCAACTGCTTAG-3′
	RP	5′-AGGTCCACCACTGACACGTT-3′
HO-1	FP	5′-TGCGGTGCAGCTCTTCTG-3′
	RP	5′-GCAACCCGACAGCATGC-3′
NQO-1	FP	5′-TGGCTAGGTATCATTCAACTC-3′
	RP	5′-CCTTAGGGCAGGTAGATTCAG-3′

Abbreviations: FP, forward sequence; RP, reverse sequence.

NOB concentrations in the blood were determined using an HPLC assay. Briefly, plasma was collected by centrifugation at 6000 g for 10 min. NOB was extracted from the plasma by acetonitrile, and tangeretin was used as an internal standard. The NOB concentrations were measured by HPLC (Shimadzu, Japan) with a C_{18} column (4.6 × 250 mm, 5 μm), using water and acetonitrile (40:60) as the mobile phase. The wavelength was set at 330 nm. Method validation was performed to determine the repeatability, stability, precision, recovery, and linear correlation according to Pharmacopoeia of the People's Republic of China (ChP, 2020). The pharmacokinetic parameters of NOB were calculated using the MaS Studio software (Mobile Application Studio, Nanjing, China).

In vivo Hepatoprotective Effects

The in vivo hepatoprotective effects of NOB/SD were investigated in APAP treated C57BL/6 mice as the acute liver injury (ALI) model. Male C57BL/6 mice (weighted 18–22 g) were randomly divided into four groups (n = 6/group). Saline, Free NOB and NOB/SD with a NOB dosage of 50 mg/kg were orally administered to mice before APAP treatment for 7 days, respectively.[9] The body weight of the mice was measured daily. On day 8, to induce acute liver injury (ALI) model, the treated mice were administrated with 350 mg/kg APAP by intraperitoneal injection.[26] Mice injected intraperitoneally with saline were used as the negative control.

At 48 h after the injection, the mice were sacrificed. Whole blood was collected, and serum was obtained by centrifugation at 3000 g for 10 min. ALT and AST in serum were measured by Chemray Biochemical Analyzer (Leidu, Shenzhen, China).[27] Liver tissues of the treated mice were collected, fixed in 4% paraformaldehyde, and accessed with the hematoxylin-eosin (H&E) staining. The prominent hepatocyte necrosis, infiltration, and inflammation were estimated from the H&E section of mice by the software image J, which were defined as the pathological areas induced by APAP. The pathological areas were expressed as the percentage of the total liver section areas.[28]

Statistical Analysis

All data shown in this study were presented as mean ± SD of at least 3 independent experiments. Data were analyzed using the GraphPad Prism 8 software (Prism, USA). Statistical analysis was performed using One-Way ANOVA, and $P < 0.05$ was considered statistical significance.

Results and Discussion

NOB Solubility in Different Polymers

To select the carriers for Solid dispersions of nobiletin (NOB/SD) preparation, the solubility of NOB in different 8 polymers including HPC, HPMC, HPMCAS, Kolliphor P407, β-CD, Soluplus, PVP K30, and PVP/VA 64 was measured. In brief, the solubility of NOB in a water-based solution containing 0.04% carrier was determined after stirring at room temperature for 5 h, and the solubility data are shown in Figure 2A. Polymers significantly improve the solubility of NOB within 300 min. Furthermore, the NOB in the polymers of Soluplus, HPC, Kolliphor P407, and PVP/VA 64 reached faster and higher solubilities than the others within 15 min. Particularly, NOB in Soluplus exhibited the highest solubility among all the selective polymers. However, these supersaturated states of NOB in polymers were unstable. The solubility

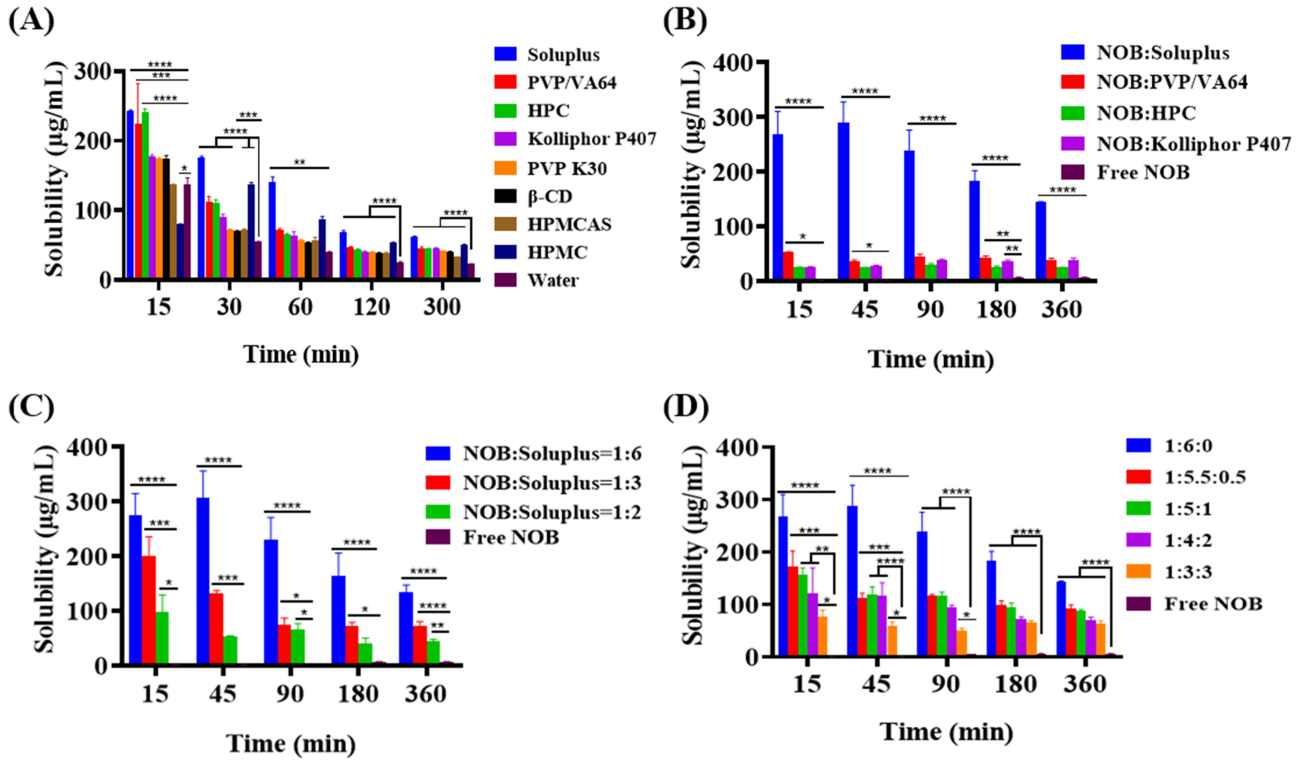

Figure 2 The solubility of NOB in different polymers and NOB/SD formulations under supersaturated condition. The solubility of NOB in different polymers and NOB/SD formulations under supersaturated condition. (**A**) The solubility of NOB in different polymers. NOB dissolved in the methanol solvent was injected into an aqueous solution containing 0.04% carrier, and the solubility of NOB was measured using a UV spectrophotometer at different time points. (**B**) The supersaturation solubility of NOB in different NOB/SD formulations with different carrier systems (including Soluplus, PVP/VA 64, HPC and Kolliphor P407) at the NOB/carrier mass ratio of 1:6. (**C**) The solubility of NOB in NOB/SD formulations with different NOB/Soluplus ratios (1:6, 1:3, 1:2, weight ratio). (**D**) The solubility of NOB in NOB/SD formulations with different NOB/Soluplus/PVP/VA 64 ratios (1:6:0, 1:5.5:0.5, 1:5:1, 1:4:2, and 1:3:3, weight ratio). In (**B**–**D**), the NOB solubility of Free NOB in water was chosen as control. NOB/SD with different formulations were prepared by SE. n = 3/group, *P<0.05; **P<0.01; ***P<0.001; ****P<0.0001.
Abbreviations: NOB, nobiletin; SE, solvent evaporation method.

of NOB in the polymers were significantly decreased with increasing incubation time. To maintain the solubility of NOB at a higher level with the incubation time increased, NOB/SD should be prepared. Therefore, the polymers including Soluplus, HPC, Kolliphor P407, and PVP/VA 64 were chosen as the carriers for NOB/SD construction, which might result in increased NOB solubility.

Preparation and Optimization of NOB/SD

Solid dispersion, which maintains insoluble drugs in amorphous states by the soluble excipient matrix, can significantly increase the drug solubility in water. The enhanced solubility of drug, attributed to its amorphous form, was significantly related to the selective excipient matrix in the formulation and the solid dispersion preparation. Therefore, the NOB/SD formulation and preparation should be optimized.

To optimize the NOB solubility in the SD formulation, NOB/SDs with different formulations were prepared using solvent evaporation method (SE) (Table 1), and the NOB solubilities generated with the solid dispersions were measured. Firstly, NOB/SDs were prepared by SE with four different single carriers (including Soluplus, PVP/PV 64, Kolliphor P407, and HPC) at a NOB/carrier mass ratio of 1:6, respectively. The solubility of NOB in different carriers showed that all the single carriers significantly improved the NOB solubility when formulated as the solid dispersions (Figure 2B). In particular, Soluplus presented the best supersaturated solubility of NOB among all the NOB/SD preparations, in which the NOB solubility was approximately 20-fold higher than that of Free NOB (Figure 2B). Meanwhile, PVP/VA 64 exhibited better NOB solubility than Kolliphor P407 and HPC (Figure 2B). Therefore, Soluplus was chosen as the drug carrier for the further solid dispersion preparations.

Then, NOB/SDs were prepared with different mass ratios of Soluplus to NOB. As shown in Figure 2C, NOB displayed an increased solubility behavior in water in a Soluplus dosage-dependent manner. In these NOB/SD systems, NOB reached rapid dissolution (274 μg/mL) for 15 min and maintained a superior supersaturation (135 μg/mL) for 6 h with an NOB/Soluplus ratio of 1:6 (mass ratio), which was 19.3 times higher than that of Free NOB (7 μg/mL) in water. The results of the solubility assay in Soluplus-based SD formulations demonstrated that Soluplus maintained NOB in a high supersaturation with a NOB/Soluplus ratio of 1:6. However, solid dispersions exhibit rapid dissolution owing to the high energy state of drug in carrier, which might also display poor physical stability with solid dispersion aging and drug recrystallization. The low glass transition temperatures (Tg) of Soluplus (approximately 64 °C) and Soluplus-based NOB/SD (approximately 64 °C) (Figure 3D and Supplement Figure 1) shown in the DSC data suggested a high energy state of NOB in Soluplus-based NOB/SD, which might result in poor physical stability including aging and drug recrystallization. The data from the physical stability assay were consistent with the DSC curves.

Our previous work demonstrated that the Tg of Soluplus could increase with the addition of PVP/VA 64, which could effectively slow down the aging of solid dispersions.[21] Herein, NOB/SDs were further optimized by different ratios of NOB/soluplus/PVP/VA 64. The results in Figure 2D indicated that NOB/SD exhibited a high supersaturation of NOB for 6 h (88 μg/mL) with a NOB/soluplus/PVP/VA 64 ratio of 1:5:1. The stability assay also evidenced that NOB/SD

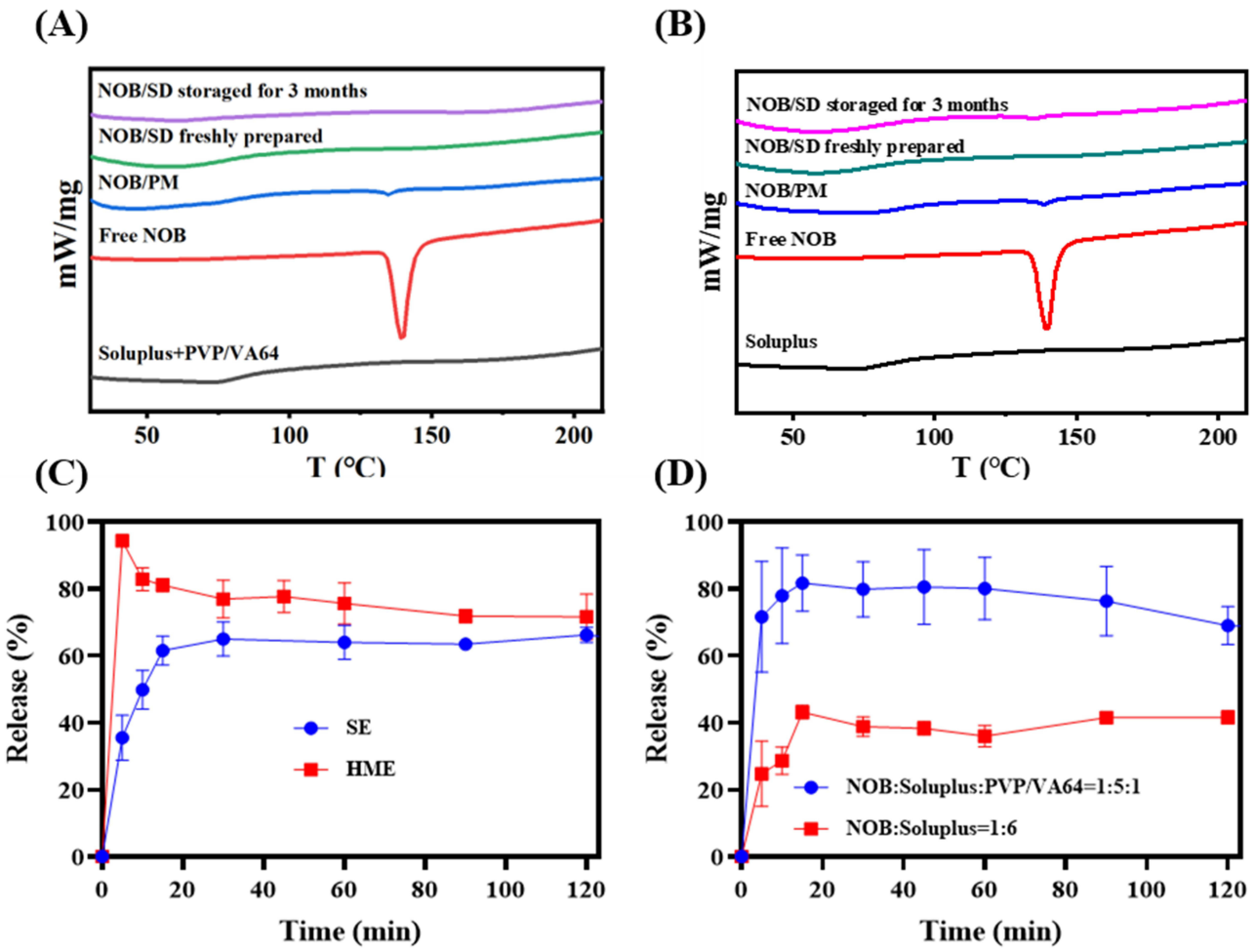

Figure 3 Physicochemical characteristics of NOB/SD formulations storage for 3 months. Physicochemical characteristics of NOB/SD formulations storage for 3 months. (**A**) DSC curves of NOB/SD formulation 8 with NOB:Soluplus:PVP/VA 64 of 1:5:1 (mass ratio) for 3 months storage. (**B**) DSC curves of NOB/SD formulation 4 with NOB: Soluplus of 1:6 (mass ratio) for 3 months storage. In (**A**) and (**B**), NOB/SD formulation 4 and 8 were prepared by HME method. Free NOB, SD carriers of Soluplus and PVP/VA 64 NOB/PM were chosen as the controls. (**C**) Dissolution curves of NOB/SD formulation 8 with NOB:Soluplus:PVP/VA 64 of 1:5:1 (mass ratio) freshly prepared by HME or SE, respectively. (**D**) Dissolution curves of NOB/SD formulation 8 with NOB:Soluplus:PVP/VA 64 of 1:5:1 (mass ratio) and NOB/SD formulation 4 with NOB:Soluplus of 1:6 (mass ratio) for 3 months storage. NOB/SD formulations were prepared by HME.

Abbreviations: NOB, nobiletin; NOB/SD, nobiletin solid dispersion; DSC, differential scanning calorimetry; HME, hot melt extrusion; SE, solvent evaporation.

formulation 8 displayed a faster and higher dissolution rate than NOB/SD formulation 4 after 3 months of storage (The results could be found in section "The physicochemical stability of NOB/SD"). Consistent with the DSC data, DSC curve showed that the Tg of NOB/SD was increased from 64.1 ºC to 79.8 °C with the addition of PVP/VA 64, which implied that NOB/SD prepared with the mixed carriers of Soluplus and PVP/VA 64 might be more stable than that of the single carrier of Soluplus (Supplement Figure 1). Therefore, the optimized NOB/SD formulation with a NOB/Soluplus/PVP/VA 64 ratio of 1:5:1 was chosen and prepared by the HME process for further investigation. Moreover, the stability of these formulations was assessed further.

Characterization of the Optimized NOB/SD Formulation

The optimized NOB/SD formulation is characterized in Figure 4. Firstly, the morphologies of Free NOB, the mixture of carriers, NOB/PM and NOB/SD were observed using SEM analysis. As shown in the SEM images in Figure 4A, blocky crystallization of NOB could be found with the particle sizes of approximately 1–5 μm in Free NOB. Moreover, some crystalline forms of NOB showed prismatic crystal structure with the particle sizes larger than 5 μm. The carrier mixture of Soluplus and PVP/VA 64 exhibited spheroid shapes and smooth surfaces. Similarly, the crystalline form of NOB with prismatic crystal structure was trapped in or attached on the carriers of NOB/PM, indicating that NOB displayed crystalline forms after physically mixing with the carriers of Soluplus and PVP/VA 64. In contrast, the prismatic crystal forms of NOB were disappeared and only a few needle-like structures were attached to the surface of the carrier in the NOB/SD. These phenomena confirmed that NOB can display

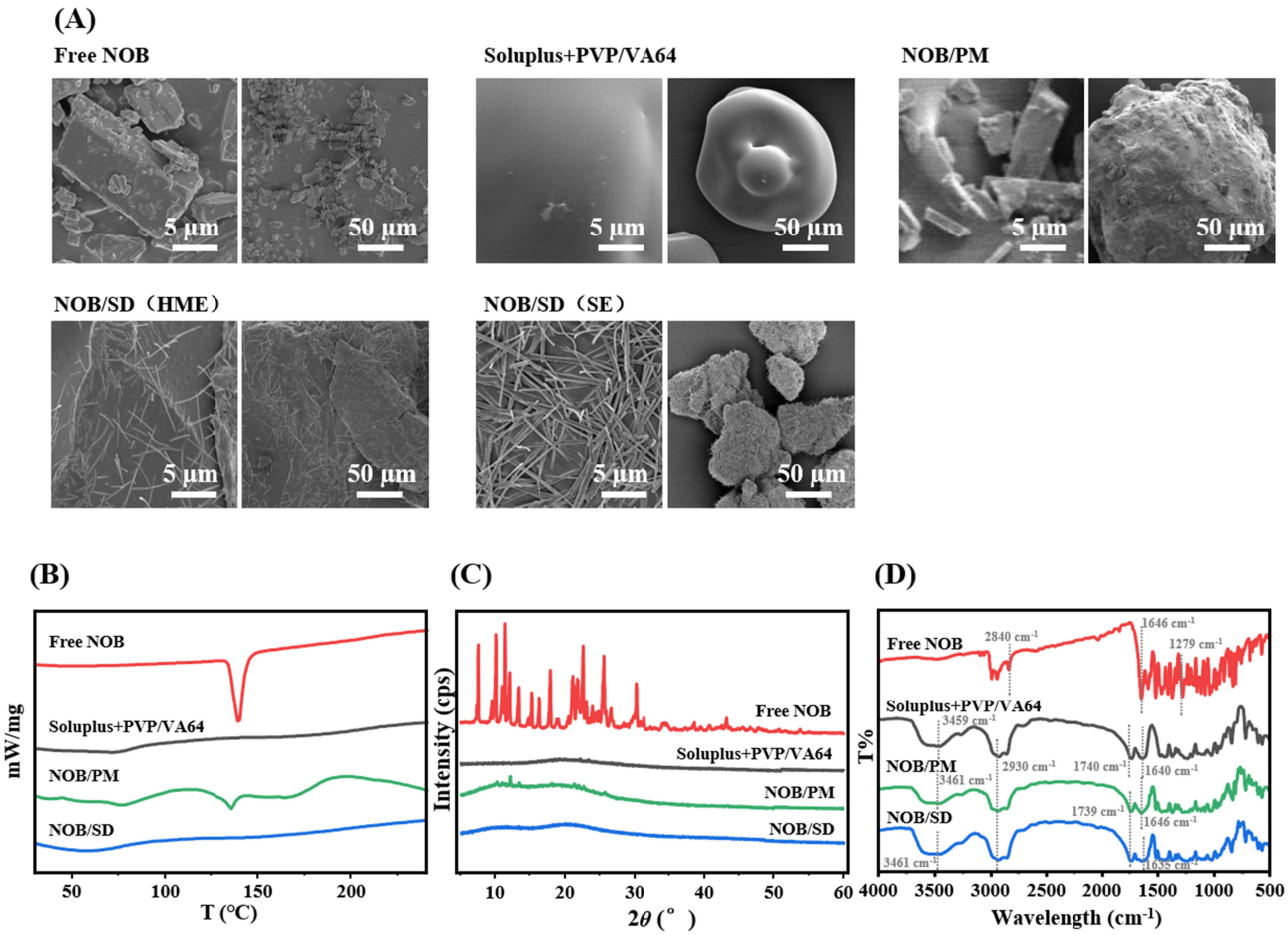

Figure 4 Physicochemical characteristics of NOB/SD. Physicochemical characteristics of NOB/SD. (**A**) SEM images of Free NOB, physical mixture of Soluplus and PVP/VA 64, NOB/PM, NOB/SD prepared by HME and NOB/SD prepared by SE. (**B**) Differential scanning calorimetry thermograms of Free NOB, mixtures of Soluplus and PVP/VA 64, NOB/PM, and NOB/SD. (**C**) Powder X-ray diffraction patterns of Free NOB, physical mixture of Soluplus and PVP/VA 64, NOB/PM, and NOB/SD. (**D**) FTIR spectra of Free NOB, physical mixture of Soluplus and PVP/VA 64, NOB/PM, and NOB/SD.

Abbreviations: NOB, nobiletin; SEM, scanning electronic microscopy; FTIR, Fourier transform infrared spectroscopy; Soluplus+PVP/VA 64, mixture of Soluplus and PVP/VA 64; NOB/PM, physical mixtures with NOB, Soluplus, and PVP/VA 64; NOB/SD, nobiletin solid dispersion prepared with Soluplus and PVP/VA 64 by HME method.

amorphous and microcrystalline states after SD technology using both the HME and SE methods. Moreover, compared with the SE method, the NOB/SD formulation prepared by HME showed fewer microcrystalline forms of NOB attachment indicating that the HME method might be superior to SE for NOB/SD preparation.[29]

To further clarify the amorphization of NOB in NOB/SD, the physicochemical properties of NOB/SD were characterized by DSC analysis. The DSC curve of Free NOB showed a sharp endothermic peak at 137 °C (Figure 4B), which could be identified as the melting point of NOB and is consistent with the DSC data reported by Wu et al.[29] The carrier mixture of Soluplus and PVP/VA 64 exhibited no endothermic peak at approximately 137 °C. In the NOB/PM system, a small endothermic peak was observed at 136 °C, indicating that NOB displayed a crystalline form in NOB/PM. In contrast, in the NOB/SD system, no crystalline endothermic peak was observed at approximately 137 °C, indicating that NOB was transformed from a crystalline form to an amorphous state after the SD process.

The physicochemical properties of the optimized NOB/SD formulations were also characterized using PXRD analysis. As shown in the PXRD curves (Figure 4C), a great deal of intense peaks ranging from 5° to 35° were observed for Free NOB, indicating the crystalline state of NOB, whereas there was no crystal diffraction peak in the carrier mixture of Soluplus and PVP/PV 64 because of their amorphous nature.[30,31] Diffraction peaks with 10°–15° and 20°–25° were still obviously observed in NOB/PM even though their intensities were weaker than those of Free NOB, which indicated the presence of NOB crystals in NOB/PM. However, the weak diffraction peaks (10°–15° and 20°–25°) were disappeared in the NOB/SD formulation, which confirmed that NOB existed an amorphous state in NOB/SD formulation.

The functional groups in the different material structures were reflected by the characteristic absorption peaks in the infrared spectrum. The formation of solid dispersion can be determined by comparing the characteristic absorption peak intensity or displacement of the drug and solid dispersion in infrared spectrum. FTIR studies were performed to elucidate the possible intermolecular interactions between NOB and the carriers. As shown in the FTIR curves (Figure 4D), the NOB molecule in Free NOB exhibited the characteristic peaks at 2840 cm^{-1} generated by the C-H stretching vibrations, 1646 cm^{-1} generated by the C=O stretching vibrations, and 1279 cm^{-1} attributed to the C-O-C stretching vibrations.[32] Soluplus and PVP/VA 64 showed wide characteristic peaks at approximately 3459 cm^{-1} generated by the O-H stretching vibrations, around 2930 cm^{-1} generated by the C-H stretching vibrations, around 1740 and 1640 cm^{-1} generated by the C=O stretching vibrations, around 1460 cm^{-1} generated by the C-O-C stretching vibrations.[33–35] NOB/PM exhibited the same wide characteristic peaks at around 3461, 2930 and 1739 cm^{-1} with the addition of PVP/VA 64. The characteristic peak at 2840 cm^{-1} were overlapped by the carriers compared with the Free NOB. The characteristic peaks at 1646 cm^{-1} corresponding to C=O were broadened with the addition of carriers (Soluplus and PVP/VA 64). NOB/SD also showed the same wide characteristic peaks at around 3461, 2930 and 1739 cm^{-1} with the addition of PVP/VA 64 compared with NOB/PM. However, the characteristic peak at 1646 cm^{-1} was shifted to 1635 cm^{-1}, which suggested that a possible hydrogen bond was formed between the proton accepting C=O groups of NOB and the proton donating –OH groups of the carriers (Soluplus and PVP/VA 64).[36] Nevertheless, the wide characteristic peaks of 3461 cm^{-1} generated by the O–H stretching vibrations could still be found in NOB/SD. This might be because the amount of the carries (Soluplus and PVP/VA 64) in the NOB/SD was more than NOB, there were plenty of free –OH of the carries left in the NOB/SD. The FTIR data demonstrated strong intermolecular interactions between NOB and carriers, which might be beneficial for the NOB solubility improvement.

The Dissolution Behavior and Solubilization Mechanism of NOB/SD

The SD products with the poor soluble drug dispersed in the hydrophilic carriers display the fast dissolution and enhanced solubility via the amorphous state of the poor soluble drug, which can improve the bioavailability and bioactivity of the drugs.[14] Herein, the fast dissolution and enhanced solubility characteristics play important roles in SD products. NOB/SD prepared with HME was supposed to improve the hepatoprotection of NOB via the fast dissolution behavior and the enhanced solubility characteristic attributed by the SD technology. Although the enhanced solubility characteristic of NOB/SD was confirmed, whether NOB/SD exhibited the fast dissolution behavior and what solubilization mechanism of NOB/SD might occur were still known. Therefore, the dissolution behavior of NOB/SD should be evaluated, and its solubilization mechanism should be clarified further.

The dissolution behavior of NOB was determined using an in vitro dissolution test. Dissolution profiles in Figure 5A showed that the release of Free NOB reached a plateau at the level of 11% after 90 min. In contrast, NOB/SD showed

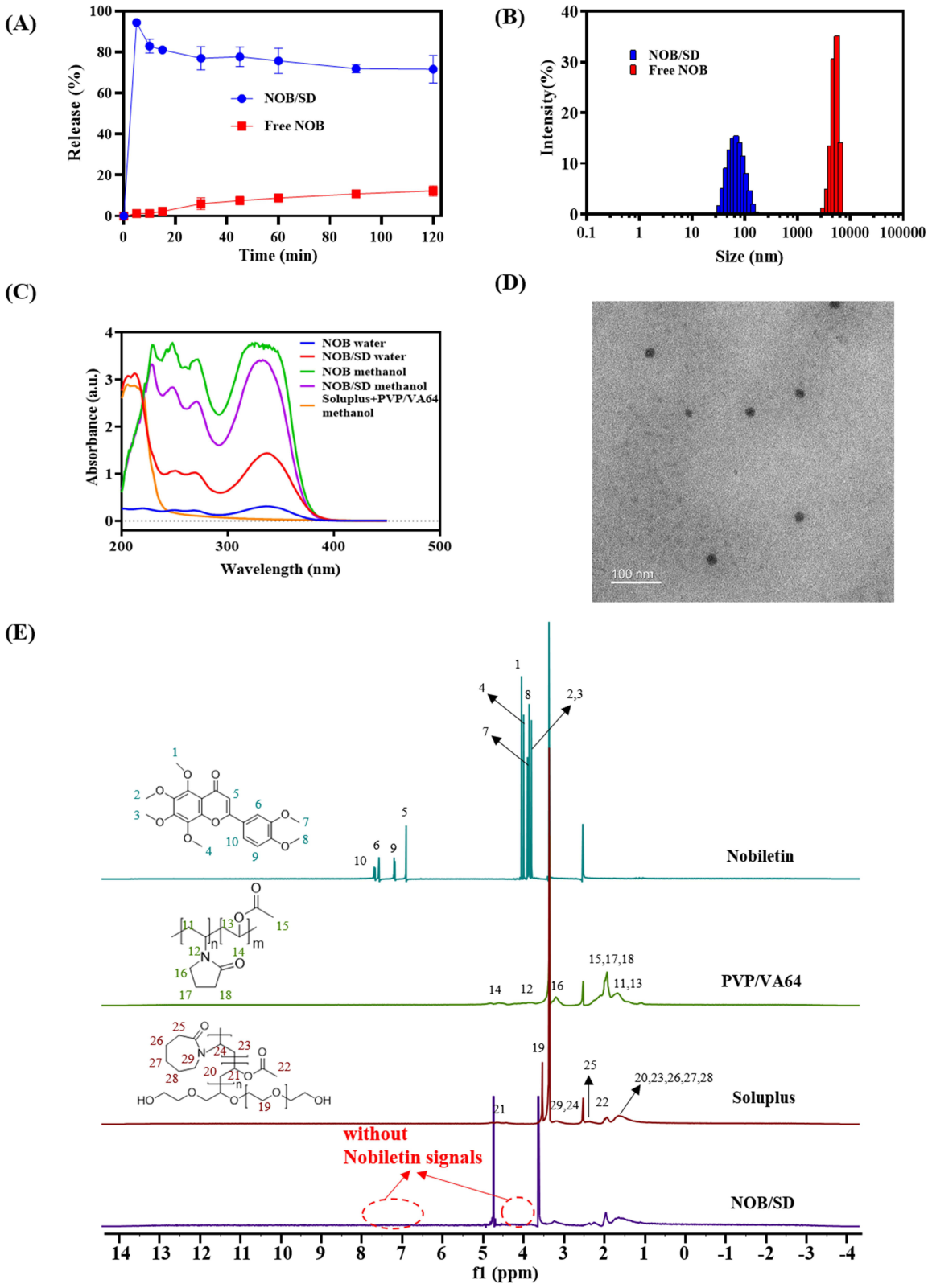

Figure 5 The dissolution behavior and solubilization mechanism of NOB/SD. The dissolution behavior and solubilization mechanism of NOB/SD. (**A**) Dissolution profiles of Free NOB and NOB/SD in PBS at pH 6.5. (**B**) Particle sizes of Free NOB and NOB/SD in water measured by DLS analysis. (**C**) UV spectra of Free NOB and NOB/SD in water or methanol. (**D**) TEM images of NOB micelles constructed by NOB/SD in water. (**E**) ^{1}H-NMR spectra of NOB, PVP/VA 64, Soluplus, and NOB/SD, respectively.
Abbreviations: NOB, nobiletin; NOB/SD, nobiletin solid dispersion; TEM, Transmission electron microscope; ^{1}H-NMR, ^{1}H nuclear magnetic resonance.

a fast and high dissolution profiles with a NOB release rate of 95% within 5 min, and maintained NOB in a supersaturated state for at least 120 min. The dissolution profiles demonstrated that NOB presented significantly enhanced dissolution behavior after the solid dispersion preparation with Soluplus and PVP/VA 64, which might be attributed to the enhanced NOB solubility in NOB/SD.

The enhanced solubilization mechanism of NOB/SD was further investigated in this study. Solid dispersions prepared using the amphipathic copolymer Soluplus and PVP/VA 64 were constructed as nano-micelles by encapsulating drugs in the core once they were dissolved in an aqueous environment.[21] Therefore, the morphology and particle size of NOB/SD in water were measured. TEM images showed that NOB/SD in water could be self-assembled into nano-micelles exhibiting spherical shapes with particle sizes of approximately 30 nm after dissolution, and no large crystals of NOB were observed (Figure 5D). The NOB micelles displayed the particle sizes of 68.64 ± 4.37 nm (PDI: 0.16 ± 0.04) by DLS analysis, which were larger than those by TEM (Table 3, Figure 5B). These might be because the particle sizes of NOB micelles measured by TEM might have volume shrinkage after the drying process of the TEM sample preparations,[37] while the particle sizes measured by DLS were the hydrated diameters of the NOB micelles dispersed in water, which might be larger than the dry diameters by TEM.[38] Conversely, Free NOB dispersed in water displayed larger particle sizes of 6581.33 ± 1089.80 nm (PDI: 1.00) according to DLS measurements. It was evidenced that NOB/SD could be self-assembled into nano-micelles by entrapping NOB in the core when dissolved in water, which induced the solubilization of NOB in the solid dispersion.

The UV spectra of NOB-based formulations dissolved in deionized water or methanol are shown in Figure 5C, respectively. Both NOB/SD and Free NOB in methanol were transparent and exhibited maximum absorption at 330 nm with the flavonoid B ring of NOB. Similar to Free NOB, NOB displayed a molecular state and was completely free when NOB/SD was dissolved in methanol, and no interaction occurred between NOB and the carriers of SD. Meanwhile, Free NOB suspended in water exhibited large amounts of NOB crystals. Free NOB exhibited a maximum absorption wavelength of 330 nm with a lower UV absorption than the other groups because of its poor solubility in water. Unlike Free NOB, NOB/SD was milky in water, exhibiting a maximum absorption wavelength shift to 337 nm. It was indicated that chemical interactions between NOB and the carriers existed in NOB/SD.

To further investigate the driving force, the micellar structure of NOB/SD was characterized by ^{1}H-NMR analysis. As shown in Figure 5E, the signals of NOB (peak 1–10) were detected in the deuterated DMSO solution, in which NOB was dissolved as free molecules. However, these signals disappeared when the NOB/SD was dissolved in D_2O. Meanwhile, signals of hydrophilic groups including the polyethylene glycol (PEG) fragment in Soluplus (peak 19) and the polyvinylpyrrolidone (PVP) fragment in PVP/VA 64 (peak 11, 13, and 14) were found in NOB/SD. These ^{1}H-NMR data confirmed the driving force interaction between NOB and the carriers of Soluplus and PVP/VA 64.

Therefore, NOB/SD exhibited enhanced NOB solubility and improved NOB dissolution behavior in water. The enhanced solubilization mechanism of NOB/SD might be attributed to the fact that the SD carriers of Soluplus and PVP/VA 64 could self-construct nano-micelles by encapsulating the hydrophobic NOB in the core once they dissolved in an aqueous environment. The promoted NOB solubility and improved NOB dissolution behavior may be beneficial for enhancing the bioavailability of NOB.

The Physicochemical Stability of NOB/SD

The stability of NOB/SD plays an important role in their biomedical applications. To investigate the stability of NOB/SD, its physicochemical stability of NOB/SD was evaluated by DSC analysis and in vitro dissolution test after 3 months of

Table 3 DLS Measurement of NOB/SD and Free NOB in Water

Formulation	Z-Average (nm)	PDI
NOB/SD	68.64±4.37	0.16±0.04
Free NOB	6581.33±1089.80	1.00±0

Abbreviation: PDI, polydispersity index.

storage at 25 °C (Figure 3). After the 3 months of storage, the NOB/SD (formulation 8 with a NOB:Soluplus:PVP/VA 64 mass ratio of 1:5:1) had no endothermic peaks at 137 °C (Figure 3A). Interestingly, a minor endothermic peak at 135 °C was observed in NOB/SD (formulation 4 with a NOB:Soluplus mass ratio of 1:6) after 3 months of storage (Figure 3B). These DSC data suggested that NOB might sustain an amorphous state in NOB/SD formulation 8 with carriers of Soluplus and PVP/VA 64, but crystallization of NOB has occurred in NOB/SD formulation 4 with carrier of Soluplus during the 3 months storage. Furthermore, SD formulation 8 prepared using HME exhibited a better dissolution behavior than SE (Figure 3C). Consistent with the DSC data, NOB/SD formulation 8 (approximately 76%) displayed a faster and higher dissolution rate than NOB/SD formulation 4 (approximately 41%) after 3 months of storage (Figure 3D).

The results of the stability investigation suggested that carriers of Soluplus and PVP/VA 64 contributed to the stronger crystallization inhibitory effects of NOB, which effectively slowed down the aging of NOB solid dispersions. The enhanced stability of NOB/SD may be useful for promoting the bioavailability and hepatoprotection of NOB.

In vitro Cellular Uptake, Biocompatibility, and Cytoprotective Effects

In the present study, the SD technology was expected to improve cellular uptake of NOB. Herein, the cellular uptake of NOB/SD in L02 cells was investigated using CLSM in vitro. The poorly water-soluble fluorescent dye C6 was entrapped in the SD carrier to track the distribution of SD in L02 cells. Cell nuclei were also stained blue with DAPI, which ensured the position of the L02 cells. As shown in Figure 6A, the cellular fluorescence intensity of C6/SD was significantly higher than that of Free C6, indicating that C6/SD showed improved cellular uptake in L02 cells compared with Free C6. The promoted cellular uptake by L02 cells might be ascribed to the self-assembly construction of C6-loaded micelles by C6/SD in the cellular culture medium, which could be beneficial for the enhanced hepatoprotection activity.[31]

To evaluate the biocompatibility of NOB and NOB/SD, the cell viabilities of L02 cells incubated with NOB and NOB/SD were detected using MTT assay, respectively. The MTT assay demonstrated that NOB and NOB/SD (NOB ranging from 3 to 12 μM) showed no significant cytotoxicity in L02 cells for 24 h, which indicated that Free NOB and NOB/SD displayed good biocompatibility in L02 cells (Figure 6B).

To investigate the in vitro cytoprotective effects of NOB/SD, the cell viabilities of Free NOB and NOB/SD on APAP-treated L02 cells were measured, respectively. As shown in Figure 6C, the cell viabilities were significantly decreased in L02 cells with APAP exposure. Interestingly, the NOB formulations including Free NOB and NOB/SD prevented the APAP-induced cytotoxicity in a NOB concentration-dependent manner (Figure 6C). Furthermore, NOB/SD displayed better cytoprotective effects than Free NOB (Figure 6C).

These results confirmed that NOB/SD displayed improved cellular uptake of NOB, good biocompatibility with L02 cells, and alleviated APAP-induced cytotoxicity in vitro.

The Anti-Apoptotic Effect and Anti-Oxidative Stress in vitro

The cytoprotective mechanisms of NOB/SD were further investigated. Oxidative stress via the nuclear factor erythroid 2-related factor (Nrf2) signaling pathway plays a pivotal role in APAP-induced hepatocytotoxicity, which induces the mRNA expression of HO-1 and NQO1 decrease, reactive oxygen species (ROS) overgeneration and cell apoptosis in APAP-stimulated cells.[23,39] Thus, the anti-apoptotic effect and anti-oxidative stress are beneficial for APAP-induced hepatocytotoxicity treatment.

Firstly, the anti-apoptotic effect of NOB/SD on APAP-stimulated L02 cells was assessed by flow cytometry using Annexin V/PI staining. As expected, the cell apoptosis accounted for 53.09 ± 3.05% after exposure to APAP (Figure 7A and B), whereas the ratios of apoptotic cells were reduced to 39.34 ± 1.05% and 23.94 ± 4.18% in Free NOB and NOB/SD (12 μM) groups, respectively (Figure 7A and B), which indicated that NOB and NOB/SD protected APAP-induced L02 cells via anti-apoptotic effect.[40] Moreover, compared with NOB, NOB/SD exhibited better cytoprotective effect against the hepatocyte damage on APAP-stimulated L02 cells.

Then, the ROS scavenging activity of NOB/SD was investigated using DCFH-DA staining. Oxidative stress stimulated by APAP might make contribution on accelerate cell aging by mitochondrial dysfunction via reactive oxygen species (ROS) overgeneration.[41] Compared with the negative controls (L02 cells without APAP treatment), the non-fluorescent probe DCFH-DA was converted to the green fluorescent dye DCFH-DA in L02 cells with APAP exposure,

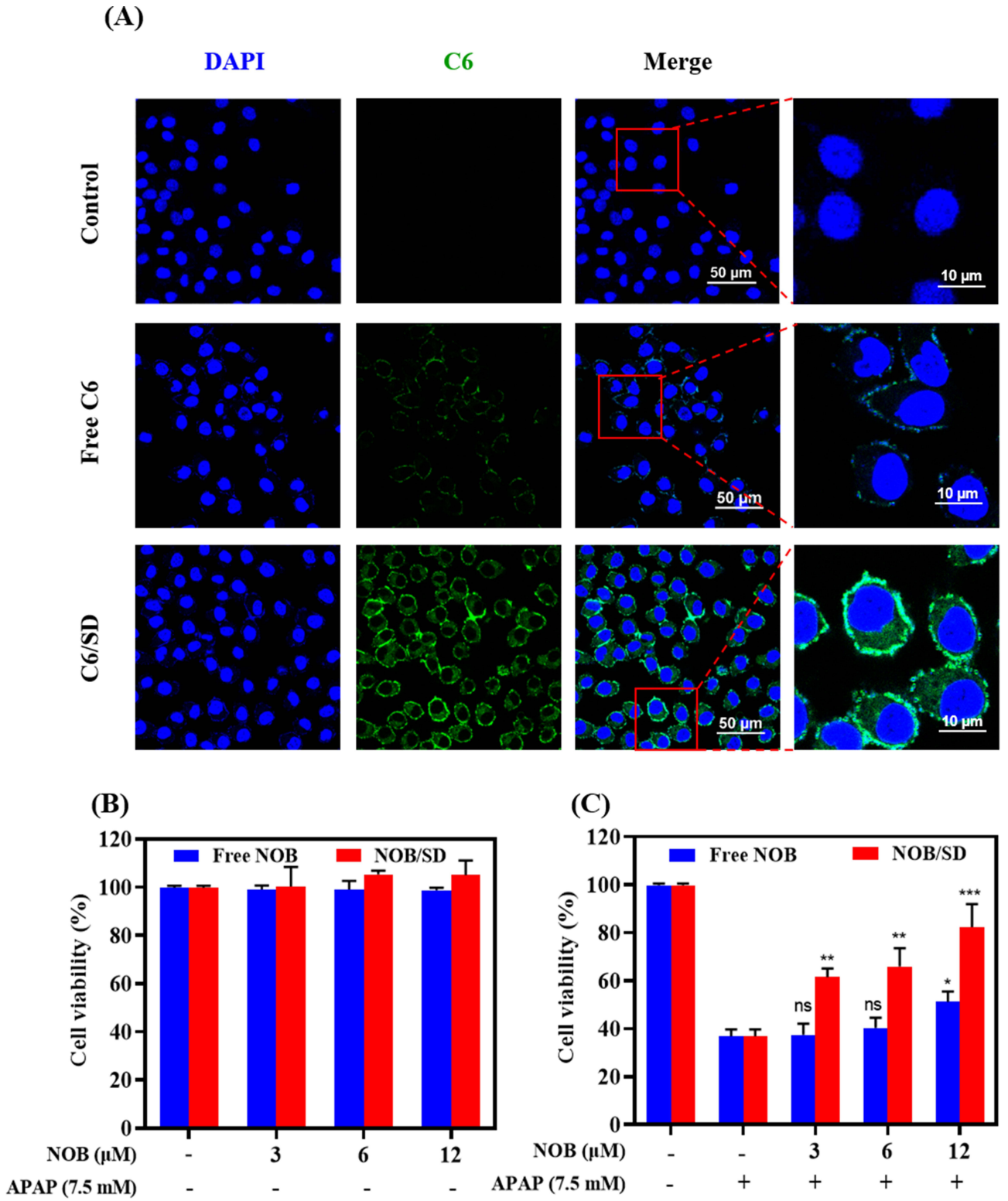

Figure 6 In vitro cellular uptake, biocompatibility, and cytoprotective activity evaluations of NOB/SD in L02 cells. In vitro cellular uptake, biocompatibility, and cytoprotective activity evaluation of NOB/SD in L02 cells. (**A**) CLSM images of L02 cells treated with C6 and C6/SD for 4 h, respectively. Cells were stained green with C6 or C6/SD, and cell nuclei were stained blue with DAPI, respectively. (**B**) Cell viabilities of L02 cells treated with Free NOB or NOB/SD for 24 h, respectively. (**C**) Cell viabilities of Free NOB and NOB/SD on APAP treated L02 cells. L02 cells were respectively incubated with Free NOB and NOB/SD at different NOB concentrations for 24 h, followed by APAP (7.5 mM) treatment for 24 h. In (**B** and **C**), the cell viabilities were analyzed by MTT assay at 570 nm. n = 3, means ± SD. * P<0.05; ** P<0.01; *** P<0.001. "ns" indicated not significant, compared with only APAP treated group.

Abbreviations: NOB, nobiletin; NOB/SD, nobiletin solid dispersion; C6, coumarin 6; C6/SD; coumarin 6 labeled solid dispersion; CLSM, confocal laser scanning microscope; APAP, acetaminophen.

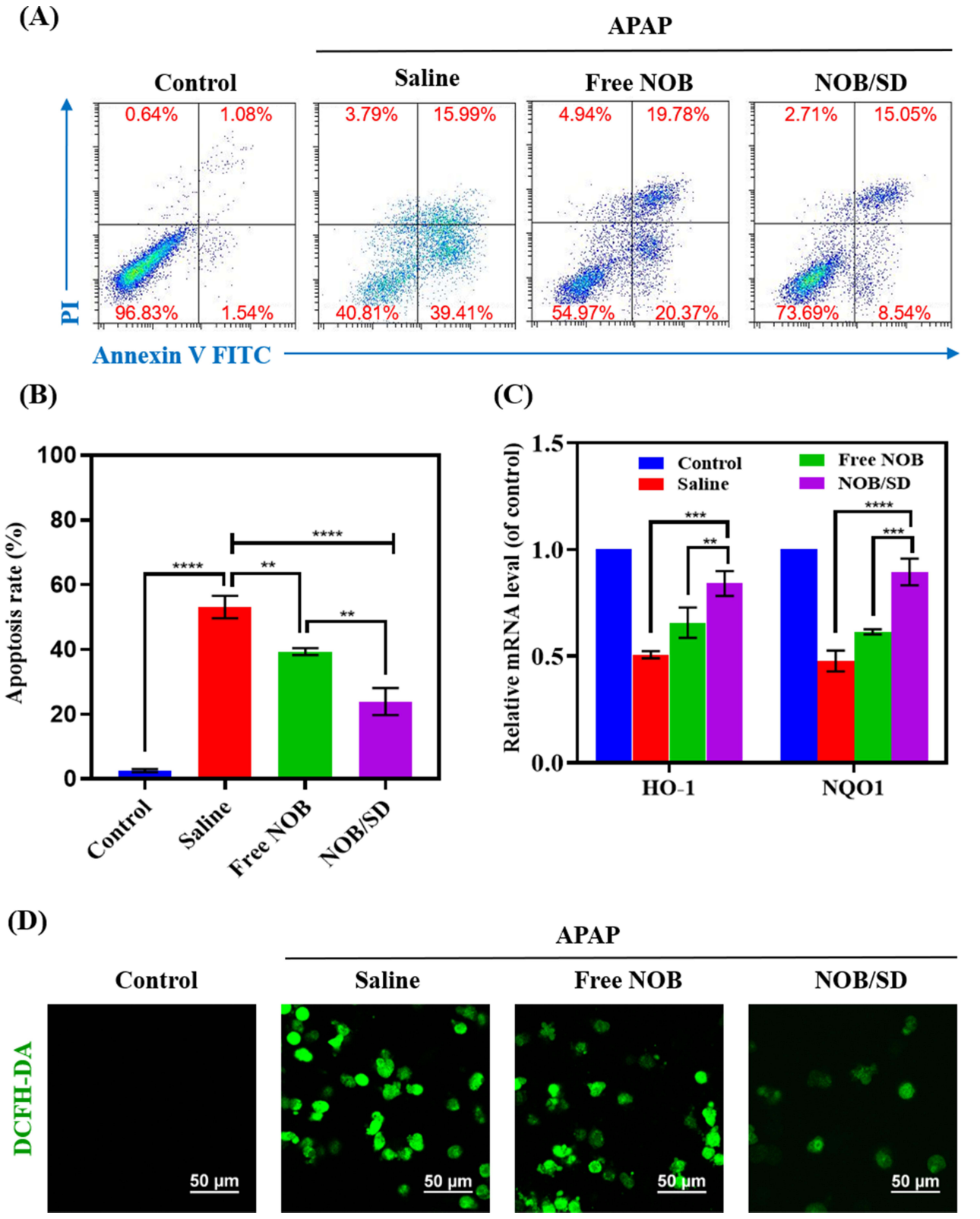

Figure 7 The evaluation of cellular anti-apoptosis and Nrf2 mediated antioxidative stress induced by NOB/SD in vitro. The evaluation of cellular anti-apoptosis and Nrf2 mediated antioxidative stress induced by NOB/SD in vitro. (**A**) The antiapoptotic effects of NOB based formulations assessed by flow cytometry with Annexin V-FITC/PI staining. (**B**) The apoptosis rates calculated by data from flow cytometry analysis. (**C**) The mRNA expression in L02 cells detected by quantitative RT-PCR. Results were normalized to GAPDH and expressed as fold change compared to the control group. (**D**) The intracellular ROS levels in L02 detected by CLSM with DCFH-DA staining as green fluorescence. n = 3/group, **P<0.01; ***P<0.001; ****P<0.0001.

Abbreviations: NOB, nobiletin; RT-PCR, reverse transcription-polymerase chain reaction; ROS, reactive oxygen species; CLSM, confocal laser scanning microscope.

indicating the ROS overgeneration on APAP-induced hepatocyte damage (Figure 7D). As anticipated, the fluorescent intensities were decreased in L02 cells pretreated with Free NOB and NOB/SD. Interestingly, the intracellular ROS levels of NOB/SD in APAP-stimulated L02 cells were remarkably lower than those of Free NOB. Therefore, NOB/SD demonstrated to have effective ROS-scavenging ability on L02 cells exposed to APAP.

Furthermore, the activation of the Nrf2 signaling pathway significantly contributes to the prevention of oxidative stress in APAP-induced liver injury. To confirm the activation of the Nrf2 signaling pathway by NOB/SD, the mRNA expression of HO-1 and NQO1 was detected by qPCR (Figure 7C). APAP significantly increased the mRNA expressions of HO-1 and NQO1, suggesting that APAP enhanced Nrf2 mediated oxidative stress in L02 cells. Free NOB and NOB/SD significantly increased the mRNA expressions of HO-1 and NQO1 ($P < 0.05$). Additionally, the mRNA expressions of HO-1 and NQO1 in NOB/SD were significantly higher than those in Free NOB, which suggested that NOB/SD attenuated APAP-induced oxidative stress by inducing the Nrf2-mediated cytoprotective enzymes of HO-1 and NQO1.[42] In order to further explore this interesting phenomenon, more supportive evidence performed by the Western blot analysis will be provided in our future work.

These results showed that NOB/SD displayed an efficient hepatoprotective effect against APAP-induced liver injury (AILI) by enhancing anti-apoptosis and improving anti-oxidative stress with ROS scavenge and Nrf2 activation. This further verified that NOB/SD protected against the APAP-induced hepatotoxicity via cellular anti-apoptosis by Nrf2 anti-oxidative stress in vitro.

In vivo Pharmacokinetics of NOB/SD

To investigate the improved bioavailability of NOB/SD, an in vivo pharmacokinetic study was performed on healthy SD rats orally administered Free NOB and NOB/SD, respectively. The plasma concentration–time profiles are shown in Figure 8F, and the pharmacokinetic parameters are calculated in Table 4. Free NOB reached the maximum plasma concentration (C_{max}) of 1.26 ± 0.51 μg/mL at approximately 0.83 h, exhibiting an area under the curve (AUC) of 2.89 ± 1.28 μg·h/mL, whereas NOB/SD reached the C_{max} of 7.23 ± 1.62 μg/mL at approximately 0.67 h, displaying an AUC of 9.68 ± 1.74 μg·h/mL.

These phenomena suggested that the C_{max} and AUC of NOB/SD were 5.74-fold and 3.25-fold higher than those of Free NOB, respectively. It was verified that NOB/SD displayed better oral bioavailability than Free NOB with its water solubility improvement by solid dispersion technology, which might achieve an enhanced hepatoprotective efficacy for AILI treatment.

In vivo Hepatoprotective Efficacy of NOB/SD

Considering the in vitro cytoprotective effects and the in vivo enhanced oral bioavailability of NOB/SD, NOB/SD may display hepatoprotective efficacy against AILI prevention in vivo. To verify the hepatoprotective efficacy of NOB/SD, an acute liver injury model was established, and the treatment protocol of NOB/SD was present (Figure 8A). C57BL/6 mice received 350 mg/kg of APAP by intraperitoneal injection, and the healthy C57BL/6 mice were orally administrated by NOB/SD with the NOB dosage of 50 mg/kg based on the previous work and our experimental data.[9,26]

Compared to the negative control (mice without APAP treatment), prominent hepatocyte necrosis and inflammatory cell infiltration were observed in the saline group with APAP treatment, suggesting liver damage caused by the APAP challenge (Figure 8B). Nevertheless, these histological abnormalities were significantly reduced by the pretreatment with Free NOB and NOB/SD for 7 days (Figure 8B). The quantitative analysis indicated that the saline group caused an H&E positive pathological area of 45% (Figure 8B). In contrast, the pre-treatment with Free NOB and NOB/SD decreased the H&E positive pathological area to 25% and 11%, respectively (Figure 8C), suggesting obvious protective effects on hepatocytes of Free NOB and NOB/SD against AILI.[43]

Plasma ALT and AST levels are the most sensitive markers of acute hepatocyte injury. Normally, plasma ALT and AST levels showed low concentrations in blood ranging from 0 to 40 U/L. ALT and AST are released from the liver cells, inducing a large amount of plasma ALT and AST, once the liver cells were damaged. As shown in Figure 8D and E, the mice treated with APAP exhibited significantly high levels of ALT (1115.43 ± 241.69 U/L) and AST (622.43 ± 69.24 U/L), respectively, suggesting the successful establishment of the acute liver injury model by APAP treatment. The ALT and

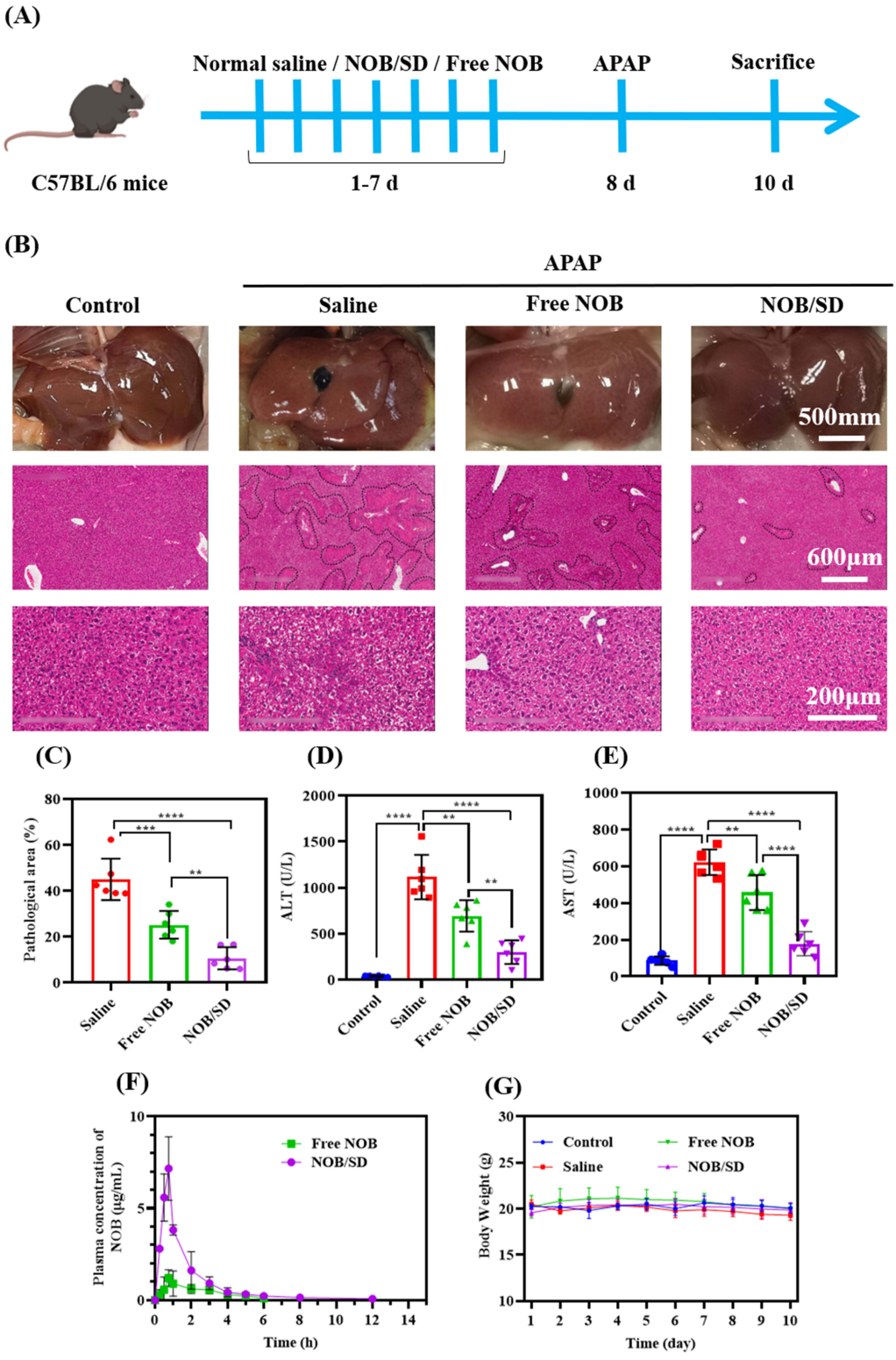

Figure 8 The in vivo hepatoprotective efficacy and bioavailability of NOB/SD. The in vivo hepatoprotective efficacy and bioavailability of NOB/SD. (**A**) The schematic illustration of APAP induced liver injury mice model and the treatment protocol of NOB. (**B**) The H&E images of liver from the APAP induced liver injury mice after different treatments. The morphologies of whole liver were shown in the upper panel (Scale bar: 500 mm). The representative HE staining images of liver sections were shown in the middle panel (Scale bar: 600 μm) and the lower panel (Scale bar: 200 μm). The pathological area was circled by the dotted line. (**C**) The quantitative analysis of liver damage by HE staining positive area with Image J software. (**D**) The plasma ALT levels from the APAP induced liver injury mice after different treatments. (**E**) The plasma AST levels from the APAP induced liver injury mice after different treatments. (**F**) The plasma concentration-time profiles of NOB in the healthy SD rats after a single oral administration of Free NOB and NOB/SD, respectively. (**G**) Body weight changes of the mice during the oral administration period of NOB/SD. n = 6/group, means±SD. **P <0.01; ***P <0.001; ****P <0.0001.
Abbreviations: HE staining, hematoxylin-eosin staining; APAP, acetaminophen; ALT, alanine aminotransferase; AST, aspartate aminotransferase.

Table 4 Pharmacokinetics Parameters of Free NOB and NOB/SD in Healthy SD Rats (n = 3)

Formulations	T_{max} (h)	C_{max} (μg/mL)	AUC_{0-12} (μg·h/mL)	Fr (%)
Free NOB	0.83±0.14	1.26±0.51	2.89±1.28	100
NOB/SD	0.67±0.14	7.23±1.62*	9.68±1.74*	325±135

Note: *P<0.05.

AST levels were significantly decreased in treatment with Free NOB (692.90 ± 170.98 and 457.53 ± 95.32 U/L) and NOB/SD (300.94 ± 128.48 U/L, 178.56 ± 65.51 U/L), respectively. The results showed that Free NOB and NOB/SD significantly reduced the APAP induced acute liver damage. Furthermore, NOB/SD exhibited more effective than Free NOB in AILI mice. Meanwhile, there was no statistically significant change in weight during the 7 days administration, indicating that NOB and NOB/SD had no obvious side effects in mice (Figure 8G).

Consequently, treatment with NOB/SD attenuated acetaminophen-induced acute liver injury in vivo without any side effects, as demonstrated by the reduced liver necrosis, decreased plasma levels of ALT and AST, and no significant change in weight. Therefore, NOB/SD displayed superior biocompatibility and desirable protective effects against AIL.

Healthy SD rats are commonly used as the animal model on the pharmacokinetic study, which provide adequate plasma for bioavailability assay, according to the references published,[44,45] while C57BL/6 mice were used to construct the acute liver injury model caused by APAP.[46–48] Moreover, the APAP-induced liver injury mice models were successfully established by C57BL/6 mice in our present works (Figure 8B–E). Therefore, the bioavailability of NOB/SD was assessed in healthy SD rats, and the in vivo hepatoprotective effects of NOB/SD were verified in C57BL/6 mice with APAP-induced liver injury.

APAP overdose-induced liver injury is a common cause of acute liver failure. Once the APAP overdose-induced liver injury (AILI) occurs, it will develop to serum alanine aminotransferase (ALT) and aspartate transaminase (AST) increase, intracellular reactive oxygen species (ROS) overgeneration, and may lead to hepatocyte necrosis, acute inflammation, or even death.[18] Traditionally, the clinical treatment for AILI was focused on alleviating the APAP-induced hepatotoxicity by the antioxidative stress with N-acetylcysteine. However, NAC therapy might suffer from adverse effects such as vomiting and allergic reactions.[6] More effective therapeutic strategies for preventing AILI are in great demand. In this present work, a novel self-assembly nano-drug delivery system of nobiletin (solid dispersion of NOB, termed as NOB/SD) was developed to alleviate the AILI, in which the amphiphilic copolymers of Soluplus and PVP/VA 64 were used to load the potential hepatoprotective agent NOB via hot melt extrusion technology (HME).

The therapeutic agents for alleviating tissue damage via cytoprotection mechanism have demonstrated to be an effective approach for different kinds of disease treatments.[49,50] Ascribed to the cytoprotection mechanism, the therapeutic agents showed great protection on tissue damages such as acute liver injury and ocular hypertension, which were attributed to the anti-apoptosis, anti-oxidative stress and ROS scavenge via Nrf2 activation. Based on the fact that NOB protects hepatocytes from necrosis by relieving oxidative stress and inflammation via NF-κB pathway, the potential hepatoprotective agent NOB was applied to prevent the APAP-induced acute liver injury in this current work.[39] The results showed that NOB could attenuate APAP-induced acute liver injury with the improved bioavailability and enhanced efficient hepatoprotection by solid dispersion technology.

Solid dispersion is a promising strategy for drug delivery. Solid dispersion with poor soluble drugs dispersed in amphiphilic copolymers could maintain drugs at amorphous states, which could improve the in vivo bioavailability and bioactivity of drugs.[16] In this current work, the novel self-assembly nano-drug delivery system NOB/SD for liver injury prevention is achieved by the solid dispersion of NOB with Soluplus and PVP/VA 64 via HME technology. NOB/SD is demonstrated to attenuate APAP-induced acute liver injury, with the following advantages. Firstly, NOB/SD could self-assembly construct to NOB micelles when dissolved in an aqueous environment. Secondly, the NOB micelles formed by NOB/SD enhance the bioavailability of NOB in vivo. Thirdly, the NOB micelles formed by NOB/SD promote the anti-apoptosis and antioxidative stress of NOB with Nrf2 activation and ROS scavenge in acute liver injury. Overall, a novel

self-assembly nano-drug delivery system NOB/SD may serve as a promising strategy to alleviate APAP-induced acute liver injury with the increased hepatoprotective efficacy.

Conclusion

In conclusion, a novel self-assembly nano drug delivery system of nobiletin (NOB/SD) was successfully developed based on solid dispersion technology. The optimized NOB/SD system was constructed using the amphiphilic copolymers of Soluplus and PVP/VA 64 by the HME method. NOB/SD could maintain NOB in a stable amorphous state with SD carriers, and then self-assembled nano-micelles with the encapsulation of NOB in the core once dissolved in an aqueous environment. The nanostructures displayed enhanced solubility, improved release behavior in vitro, and enhanced bioavailability of NOB in vivo. NOB/SD also showed enhanced cellular uptake, promoted anti-apoptosis, and alleviated the APAP-induced liver injury by improving anti-oxidative stress via ROS scavenge and Nrf2 activation. Therefore, NOB/SD might have great potential in attenuating APAP-induced acute liver injury with efficient hepatoprotection, which could be a promising hepatoprotective nano-drug delivery system for the prevention of APAP-induced acute liver injury.

Acknowledgments

This research was supported by the Guangdong Basic and Applied Basic Research Foundation (No. 2021A1515220188), the Undergraduate Teaching Quality and Teaching Reform Project Construction Project of Guangdong Province in 2022 (YJGH[2023] No.4), the Graduate Education Innovation Program Project of Guangdong Province in 2023 (YJYH[2023] No.3), Student Innovation Ability Improvement Program of Guangzhou Medical University (2023) (02-408-2304-13054XM), and the High-level University Construction Fund of Guangdong Province (02-410-2206275), (02-445-2301208XM).

Disclosure

The authors declare no conflicts of interest in this work.

References

1. Dai C, Xiao X, Li D, et al. Chloroquine ameliorates carbon tetrachloride-induced acute liver injury in mice via the concomitant inhibition of inflammation and induction of apoptosis. *Cell Death Dis*. 2018;9(12):1164. doi:10.1038/s41419-018-1136-2
2. Ghanem CI, Perez MJ, Manautou JE, et al. Acetaminophen from liver to brain: new insights into drug pharmacological action and toxicity. *Pharmacol Res*. 2016;109:119–131. doi:10.1016/j.phrs.2016.02.020
3. Friedrich M, Akimova E, Huf W, et al. Drug-induced liver injury during anti-depressant treatment: results of AMSP, a drug surveillance program. *Int J Neuropsychoph*. 2016;19(4):yv126. doi:10.1093/ijnp/pyv126
4. Licata A, Minissale MG, Stankeviciute S, et al. N-acetylcysteine for preventing acetaminophen-induced liver injury: a comprehensive review. *Front Pharmacol*. 2022;13:828565. doi:10.3389/fphar.2022.828565
5. Sanabria-Cabrera J, Tabbai S, Niu H, et al. N-Acetylcysteine for the management of non-acetaminophen drug-Induced liver injury in adults: a systematic review. *Front Pharmacol*. 2022;13:876868. doi:10.3389/fphar.2022.876868
6. Gao RY, Wang M, Liu Q, et al. Hypoxia-inducible factor-2alpha reprograms liver macrophages to protect against acute liver injury through the production of interleukin-6. *Hepatology*. 2020;71(6):2105–2117. doi:10.1002/hep.30954
7. Chagas M, Behrens MD, Moragas-Tellis CJ, et al. Flavonols and flavones as potential anti-inflammatory, antioxidant, and antibacterial compounds. *Oxid Med Cell Longev*. 2022;2022:9966750. doi:10.1155/2022/9966750
8. Hosokawa Y, Hosokawa I, Ozaki K, et al. Nobiletin inhibits inflammatory reaction in interleukin-1β-stimulated human periodontal ligament cells. *Pharmaceutics*. 2021;13(5):667. doi:10.3390/pharmaceutics13050667
9. Wu Y, Zhang W, Li M, et al. Nobiletin ameliorates ischemia-reperfusion injury by suppressing the function of Kupffer cells after liver transplantation in rats. *Biomed Pharmacother*. 2017;89:732–741. doi:10.1016/j.biopha.2017.02.087
10. Yang CJ, Nguyen DD, Lai JY. Poly(l-Histidine)-mediated on-demand therapeutic delivery of roughened ceria nanocages for treatment of chemical eye injury. *Adv Sci*. 2023;e2302174. doi:10.1002/advs.202302174
11. Lou SN, Lin YS, Hsu YS, et al. Soluble and insoluble phenolic compounds and antioxidant activity of immature calamondin affected by solvents and heat treatment. *Food Chem*. 2014;161:246–253. doi:10.1016/j.foodchem.2014.04.009
12. Onozuka H, Nakajima A, Matsuzaki K, et al. Nobiletin, a citrus flavonoid, improves memory impairment and abeta pathology in a transgenic mouse model of Alzheimer's disease. *J Pharmacol Exp Ther*. 2008;326(3):739–744. doi:10.1124/jpet.108.140293
13. Nguyen DD, Lai J. Synthesis, bioactive properties, and biomedical applications of intrinsically therapeutic nanoparticles for disease treatment. *Chem Eng J*. 2022;435:134970. doi:10.1016/j.cej.2022.134970
14. Fu J, Liu C. Tri-block polymer with interfacial layer formation ability and its use in maintaining supersaturated drug solution after dissolution of solid dispersions. *Int J Nanomedicine*. 2018;13:1611–1619. doi:10.2147/IJN.S152415

15. Kim M, Kim J, Park HJ, et al. Enhanced bioavailability of sirolimus via preparation of solid dispersion nanoparticles using a supercritical antisolvent process. *Int J Nanomedicine*. 2011;6:2997–3009. doi:10.2147/IJN.S26546
16. Sun X, Zhu D, Cai Y, et al. One-step mechanochemical preparation and prominent antitumor activity of SN-38 self-micelle solid dispersion. *Int J Nanomedicine*. 2019;14:2115–2126. doi:10.2147/IJN.S193783
17. Li J, Li C, Zhang H, et al. Preparation of azithromycin amorphous solid dispersion by hot-melt extrusion: an advantageous technology with taste masking and solubilization effects. *Polymers*. 2022;14(3):495. doi:10.3390/polym14030495
18. Ren T, Chen J, Qi P, et al. Goserelin/PLGA solid dispersion used to prepare long-acting microspheres with reduced initial release and reduced fluctuation of drug serum concentration in vivo. *Int J Pharm*. 2022;615:121474. doi:10.1016/j.ijpharm.2022.121474
19. Triboandas H, Pitt K, Bezerra M, et al. Itraconazole amorphous solid dispersion tablets: formulation and compaction process optimization using quality by design principles and tools. *Pharmaceutics*. 2022;14(11):2398. doi:10.3390/pharmaceutics14112398
20. Agafonov M, Ivanov S, Terekhova I. Improvement of pharmacologically relevant properties of methotrexate by solid dispersion with pluronic F127. *Mater Sci Eng C Mater Biol Appl*. 2021;124:112059. doi:10.1016/j.msec.2021.112059
21. Wei M-Y, Lei X-P, Fu -J-J, et al. The use of amphiphilic copolymer in the solid dispersion formulation of nimodipine to inhibit drug crystallization in the release media: combining nano-drug delivery system with solid preparations. *Mater Sci Eng C Mater Biol Appl*. 2020;111:110836. doi:10.1016/j.msec.2020.110836
22. Zhao Y, Kao CP, Liao CR, et al. Chemical compositions, chromatographic fingerprints and antioxidant activities of Citri Exocarpium Rubrum (Juhong). *Chin Med*. 2017;12(1):16. doi:10.1186/s13020-017-0127-z
23. Li S, Li X, Chen F, et al. Nobiletin mitigates hepatocytes death, liver inflammation, and fibrosis in a murine model of NASH through modulating hepatic oxidative stress and mitochondrial dysfunction. *J Nutr Biochem*. 2022;100:108888. doi:10.1016/j.jnutbio.2021.108888
24. Yang R, Song C, Chen J, et al. Limonin ameliorates Acetaminophen-induced hepatotoxicity by activating Nrf2 antioxidative pathway and inhibiting NF-κB inflammatory response via upregulating Sirt1. *Phytomedicine*. 2020;69:153211. doi:10.1016/j.phymed.2020.153211
25. Dusabimana T, Kim SR, Kim HJ, et al. Nobiletin ameliorates hepatic ischemia and reperfusion injury through the activation of SIRT-1/FOXO3a-mediated autophagy and mitochondrial biogenesis. *Exp Mol Med*. 2019;51(4):1–16. doi:10.1038/s12276-019-0245-z
26. Lewis PS, Campana L, Aleksieva N, et al. Alternatively activated macrophages promote resolution of necrosis following acute liver injury. *J Hepatol*. 2020;73(2):349–360. doi:10.1016/j.jhep.2020.02.031
27. Onoue S, Nakamura T, Uchida A, et al. Physicochemical and biopharmaceutical characterization of amorphous solid dispersion of nobiletin, a citrus polymethoxylated flavone, with improved hepatoprotective effects. *Eur J Pharm Sci*. 2013;49(4):453–460. doi:10.1016/j.ejps.2013.05.014
28. Gao Z, Yi W, Tang J, et al. Urolithin A protects against Acetaminophen-induced liver injury in mice via sustained activation of Nrf2. *Int J Biol Sci*. 2022;18(5):2146–2162. doi:10.7150/ijbs.69116
29. Wu D, Liang Y, Pei Y, et al. Plant exine capsules based encapsulation strategy: a high loading and long-term effective delivery system for nobiletin. *Food Res Int*. 2020;127:108691. doi:10.1016/j.foodres.2019.108691
30. Reis I, Viana JR, de Oliveira NJ, et al. Synthesis, characterization, and thermal and computational investigations of the L-histidine bis(fluoride) crystal. *J Mol Model*. 2022;28(8):222. doi:10.1007/s00894-022-05168-x
31. Hanumantharao R, Kalainathan S. Growth and spectroscopic investigation of a new crystal for NLO applications: $C_{10}H_{20}KN_5O_9$. *Spectrochim Acta A Mol Biomol Spectrosc*. 2012;99:181–188. doi:10.1016/j.saa.2012.09.030
32. Wang Y, Cui W, Pang G, et al. Analyses of physical and chemical compositions of different medicinal specifications of CRPV by use of multiple instrumental techniques combined with multivariate statistical analysis. *Molecules*. 2022;27(10):3285. doi:10.3390/molecules27103285
33. Costa BLA, Sauceau M, Del Confetto S, et al. Determination of drug-polymer solubility from supersaturated spray-dried amorphous solid dispersions: a case study with Efavirenz and Soluplus®. *Eur J Pharm Biopharm*. 2019;142:300–306. doi:10.1016/j.ejpb.2019.06.028
34. Zi P, Zhang C, Jun C, et al. Solubility and bioavailability enhancement study of lopinavir solid dispersion matrixed with a polymeric surfactant-Soluplus. *Eur J Pharm Sci*. 2019;134:233–245. doi:10.1016/j.ejps.2019.04.022
35. Song Y, Wang L, Yang P, et al. Physicochemical characterization of Felodipine-Kollidon VA64 amorphous solid dispersions prepared by hot-melt extrusion. *J Pharm Sci*. 2013;102(6):1915–1923. doi:10.1002/jps.23538
36. Lavra ZM, Santana DP, Re MI. Solubility and dissolution performances of spray-dried solid dispersion of Efavirenz in Soluplus®. *Drug Dev Ind Pharm*. 2017;43(1):42–54. doi:10.1080/03639045.2016.1205598
37. He H, Ren Y, Wang Z, et al. A pH-responsive poly(ether amine) micelle with hollow structure for controllable drug release. *RSC Adv*. 2016;6(94):91940–91948. doi:10.1039/C6RA18555J
38. Jia N, Ye Y, Wang Q, et al. Preparation and evaluation of poly(l-histidine) based pH-sensitive micelles for intracellular delivery of doxorubicin against MCF-7/ADR cells. *Asian J Pharm Sci*. 2017;12(5):433–441. doi:10.1016/j.ajps.2017.05.007
39. Guvenc M, Cellat M, Gokcek İ, et al. Nobiletin attenuates Acetaminophen-induced hepatorenal toxicity in rats. *J Biochem Mol Toxicol*. 2020;34(2):e22427. doi:10.1002/jbt.22427
40. Shu Y, He D, Li W, et al. Hepatoprotective effect of Citrus aurantium L. Against APAP-induced liver injury by regulating liver lipid metabolism and apoptosis. *Int J Biol Sci*. 2020;16(5):752–765. doi:10.7150/ijbs.40612
41. Chen Z, Tian R, She Z, et al. Role of oxidative stress in the pathogenesis of nonalcoholic fatty liver disease. *Free Radic Biol Med*. 2020;152:116–141. doi:10.1016/j.freeradbiomed.2020.02.025
42. Joshi A, Upadhyay KK, Vohra A, et al. Melatonin induces Nrf2-HO-1 reprogramming and corrections in hepatic core clock oscillations in non-alcoholic fatty liver disease. *FASEB J*. 2021;35(9):e21803. doi:10.1096/fj.202002556RRR
43. Lin ZH, Chan YF, Pan MH, et al. Aged Citrus Peel (Chenpi) prevents Acetaminophen-induced hepatotoxicity by epigenetically regulating Nrf2 pathway. *Am J Chin Med*. 2019;47(08):1833–1851. doi:10.1142/S0192415X19500939
44. Ren S, Jiao L, Yang S, et al. A novel co-crystal of bexarotene and ligustrazine improves pharmacokinetics and tissue distribution of bexarotene in SD rats. *Pharmaceutics*. 2020;13(1):12. doi:10.3390/pharmaceutics13010012
45. Li C, Song X, Song J, et al. Pharmacokinetic study of gallocatechin-7-gallate from Pithecellobium clypearia Benth in rats. *Acta Pharm Sin B*. 2016;6(1):64–70. doi:10.1016/j.apsb.2015.10.001
46. Hu C, Ye J, Zhao L, et al. 5,7,3',4'-flavan-on-ol (taxifolin) protects against Acetaminophen-induced liver injury by regulating the glutathione pathway. *Life Sci*. 2019;236:116939. doi:10.1016/j.lfs.2019.116939

47. Hu C, Chen Y, Cao Y, et al. Metabolomics analysis reveals the protective effect of quercetin-3-O-galactoside(Hyperoside) on liver injury in mice induced by Acetaminophen. *J Food Biochem*;2020. e13420. doi:10.1111/jfbc.13420
48. He X, Kang K, Pan D, et al. FTY720 attenuates APAP-induced liver injury via the JAK2/STAT3 signaling pathway. *Int J Mol Med*. 2022;49(4):49. doi:10.3892/ijmm.2022.5104
49. Luo LJ, Nguyen DD, Lai JY. Harnessing the tunable cavity of nanoceria for enhancing Y-27632-mediated alleviation of ocular hypertension. *Theranostics*. 2021;11(11):5447–5463. doi:10.7150/thno.54525
50. Nguyen DD, Luo LJ, Yang CJ, et al. Highly retina-Permeating and long-acting resveratrol/metformin nanotherapeutics for enhanced treatment of macular degeneration. *ACS Nano*. 2023;17(1):168–183. doi:10.1021/acsnano.2c05824